European Journal of Medicinal Chemistry 54 (2012) 804–812

Contents lists available at SciVerse ScienceDirect

European Journal of Medicinal Chemistry

journal homepage: http://www.elsevier.com/locate/ejmech

Original article

# Biomimetic *in vitro* oxidation of lapachol: A model to predict and analyse the *in vivo* phase I metabolism of bioactive compounds

Michael Niehues [a], Valéria Priscila Barros [a], Flávio da Silva Emery [a], Marcelo Dias-Baruffi [a], Marilda das Dores Assis [b], Norberto Peporine Lopes [a,*]

[a] Faculdade de Ciências Farmacêuticas de Ribeirão Preto, Universidade de São Paulo, Av. do Cafe S/N, 14040-903 Ribeirao Preto, SP, Brazil
[b] Departamento de Química, Faculdade de Filosofia, Ciências e Letras de Ribeirão Preto, Universidade de São Paulo, SP, Brazil

ARTICLE INFO

*Article history:*
Received 19 January 2012
Received in revised form
20 June 2012
Accepted 21 June 2012
Available online 28 June 2012

*Keywords:*
Lapachol
Naphtoquinones
Biomimetic oxidation
Jacobsen catalyst
Drug metabolism
Phase I metabolism

ABSTRACT

The bioactive naphtoquinone lapachol was studied *in vitro* by a biomimetic model with Jacobsen catalyst (manganese(III) salen) and iodosylbenzene as oxidizing agent. Eleven oxidation derivatives were thus identified and two competitive oxidation pathways postulated. Similar to Mn(III) porphyrins, Jacobsen catalyst mainly induced the formation of *para*-naphtoquinone derivatives of lapachol, but also of two *ortho*-derivatives. The oxidation products were used to develop a GC–MS (SIM mode) method for the identification of potential phase I metabolites *in vivo*. Plasma analysis of Wistar rats orally administered with lapachol revealed two metabolites, α-lapachone and dehydro-α-lapachone. Hence, the biomimetic model with a manganese salen complex has evidenced its use as a valuable tool to predict and elucidate the *in vivo* phase I metabolism of lapachol and possibly also of other bioactive natural compounds.


## 1. Introduction

The prediction and elucidation of drug metabolites is a relevant step in drug development. One of the main elimination pathways for drugs, especially non-polar compounds, in the human body consists in the biotransformation of compounds by oxidation reactions catalysed by enzymes of the cytochrome P450 (CYP) superfamily, also known as phase I metabolism [1]. For that scenario several biomimetic enzymatic and non-enzymatic models have been described, although lastly none of these systems was able to adequately mimic the totality of CYP-mediated reactions [2]. However, a widely used chemical model is based on synthetic metalloporphyrins in presence of monooxygen donors, which basically mimic the iron(III) peroxo and iron(IV) oxo intermediates in the catalytic cycle of CYP 450 [3,4]. Several studies have reported potential oxidative metabolites of bioactive compounds, revealing that epoxidation, aliphatic and aromatic hydroxylation or oxidation of the heteroatoms are the most common reactions [5–8]. With regard to lapachol, a recent study on its biomimetic oxidation with a manganese(III) porphyrin complex and $H_2O_2$ as oxidizing agent, presented five oxidation products and a selectivity in the catalysis to generate *para*-naphtoquinones [9]. Other biomimetic models, such as Fenton's reagent or electrochemical induced oxidation were also shown to be interesting tools for the prediction of phase I metabolites [10,11]. In the past years metal salen complexes such as the Jacobsen catalyst (Mn(salen)), have received increasing attention as biomimetic model compounds for the active site of CYP 450. With respect to their electronic structure and catalytic activities, metallosalen complexes exhibit similar features to metalloporphyrins, catalysing usually epoxidation reactions [12]. Until now two species could be characterized by tandem mass spectrometry as the principal oxidation intermediates of the Mn(salen) with PhIO: the oxomanganese(V) complex as the actual oxygen transfer agent in epoxidation reactions, and the dimeric μ-oxo bridged with two terminal iodosylbenzene ligands which acts as reservoir species [13,14] Carbamazepine and primidone are two clinically used pharmaceuticals, on which this system was tested and successfully demonstrated as being a useful tool for the prediction of the *in vivo* drug metabolism [7,15].

Lapachol (**1**) (Fig. 1), 2-hydroxy-3-(3-methyl-2-butenyl)-1,4-naphthoquinone, is a natural occurring naphtoquinone present in several vegetal species, mainly in ones from the Bignoniaceae family

* Corresponding author. Tel.: +55 16 36024168.
*E-mail address:* npelopes@fcfrp.usp.br (N.P. Lopes).

0223-5234/$ – see front matter © 2012 Elsevier Masson SAS. All rights reserved.
http://dx.doi.org/10.1016/j.ejmech.2012.06.042

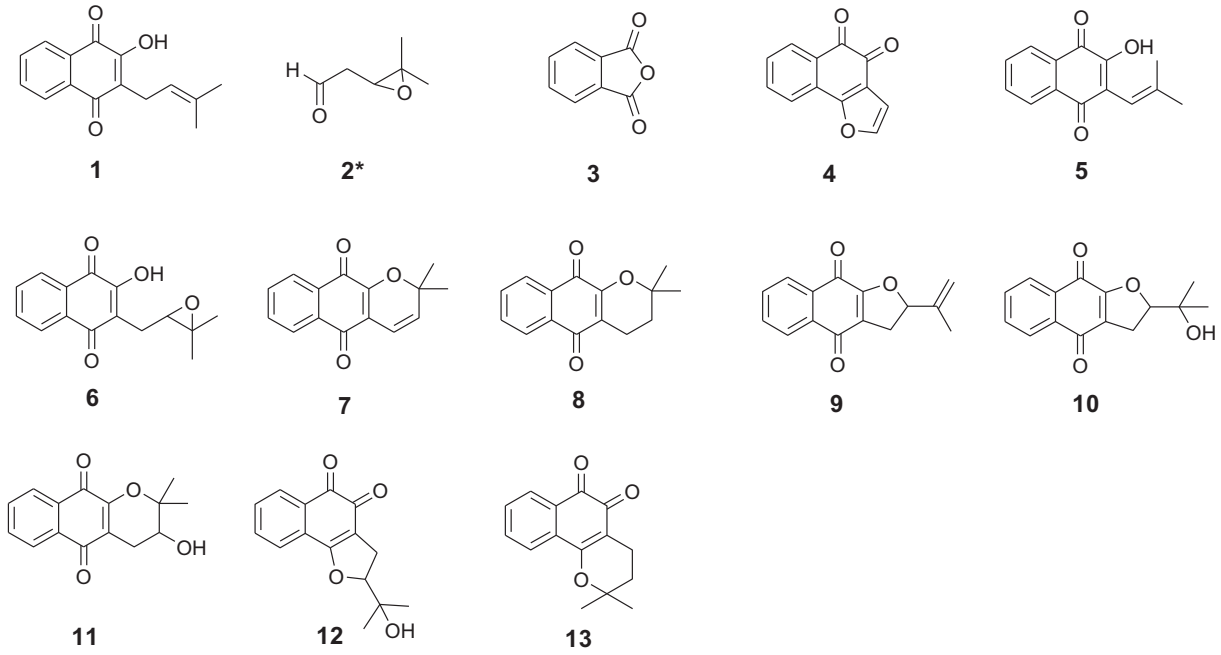


**Fig. 1.** Chemical structures of lapachol (**1**) and derivatives (**2**–**13**). Compound **2** is labelled with *, since it has only been determined by mass spectrometry (EI). Compound **13** is a synthetic derivative used to develop a GC–MS method in order to monitor putative *in vivo* metabolites of **1**.

(*Tabebuia* sp.) [16]. Many biological activities are reported, among which the cytotoxic effects against different cancer types and the trypanocidal activity may be considered as the most prominent ones [17–20]. Other interesting bioactivities of lapachol, such as against malaria or antiviral and moluscicidal activity, are resumed in the recent review by Lemos et al. [21]. Due to its anti-cancer activity early clinical studies were performed, but drug development stopped due to toxic side effects of the naphtoquinone within administered active dosages and insufficient plasma concentration levels [22]. Even so, lapachol was temporarily used in Brazil as coadjuvant in the treatment of certain cancer types [23]. The main biological interest of lapachol can therefore be centralized on its cytotoxicity by mechanisms of oxidative stress induction, thereby generating reactive oxygen species, and also of alkylation of cellular nucleophiles [24,25]. For that reason and in order to reduce unwanted toxicity as well as to improve activity, several synthetic derivatives of lapachol have been reported [26–28].

Even though lapachol has been intensively studied and already passed by pre-clinical and clinical experiments, there still is no published evidence for its metabolism in animals or humans. Consequently, the identification of further *in vitro* oxidation metabolites as well as the detailed elucidation of the *in vivo* metabolism is of great importance for this naphtoquinone. In addition, isolated oxidation derivatives enable the development of quantitative hyphenated techniques to determine pharmacokinetic and pharmacodynamic parameters of lapachol. Having said this, the present study focuses on the identification, isolation of oxidation derivatives by the biomimetic model with Mn(salen) and the development of analytical methods for the elucidation of the phase I metabolism.

## 2. Results and discussion

### 2.1. In vitro oxidation of lapachol

The first step for the identification and isolation of oxidation derivatives is the definition of the adequate catalysis conditions. Hence, the objective is to improve the proportion between lapachol, Mn(salen) and iodosylbenzene (PhIO) as terminal oxygen donor, in order to obtain high yields. Due to the reactivity of lapachol, excess of PhIO showed a negative influence on product yields, since most of the substrate was consumed and decomposed. Milder conditions with proportions of 1:30:30 (catalyst/substrate/oxidant) resulted in the formation of several products with acceptable yields and showed that lapachol was consumed by approximately 90% after 24 h.

The reaction was monitored by a GC–MS method, revealing a series of peaks of which at least eleven (peaks 2–12) could be assigned as oxidation products from lapachol (**1**) (Fig. 2). A first analysis of the processed electron ionization (EI) mass spectra for the respective peaks in conjunction with the NIST mass spectral library, V.8.0 (National Institute of Standards and Technology, Gaithersburg, MD, USA), and Wiley Registry of Mass Spectral data, 7th ed. (Wiley, Hoboken, NJ, USA), showed the presence of common cyclized pyranic derivatives in the reaction mixture, dehydro-$\alpha$-lapachone (**7**) and $\alpha$-lapachone (**8**) (Figs. 1 and 2A). Furthermore, peak **9** showed a characteristic spectrum for the isomeric furanic derivative dehydro-$\alpha$-isolapachone (**9**), with a base peak at *m/z* 197 along with a prominent fragment at *m/z* 212 [29]. The mass spectra of peaks numbered with 3–5 showed high probabilities (>90%) in the spectra libraries for other previously reported compounds, namely phtalic anhydride (**3**), naphtho[1,2-*b*]furan-4,5-dione (**4**) and norlapachol (**5**) (Figs. 1 and 2A). The EI fragmentation (70 eV) of **9** for instance showed a low intensity ion at *m/z* 199 and a molecular peak $[M]^+$ at *m/z* 198, which is well in accordance with data from literature and was confirmed by its exact mass experiment (error < 20 ppm) [30]. Peak **2** is suggested to be 3,4-epoxy-4-methylpentanal (**2**), as reported by comparison of the EI-MS fragmentation spectra (see supplementary material) to recent data from another biomimetic study with lapachol [9]. However, the isolation did not succeed and the determination of spectroscopic data will be necessary to fully confirm the suggested structure of **2**.

In despite of the value of EI mass spectra and related libraries, no additional products could therewith be identified and apart

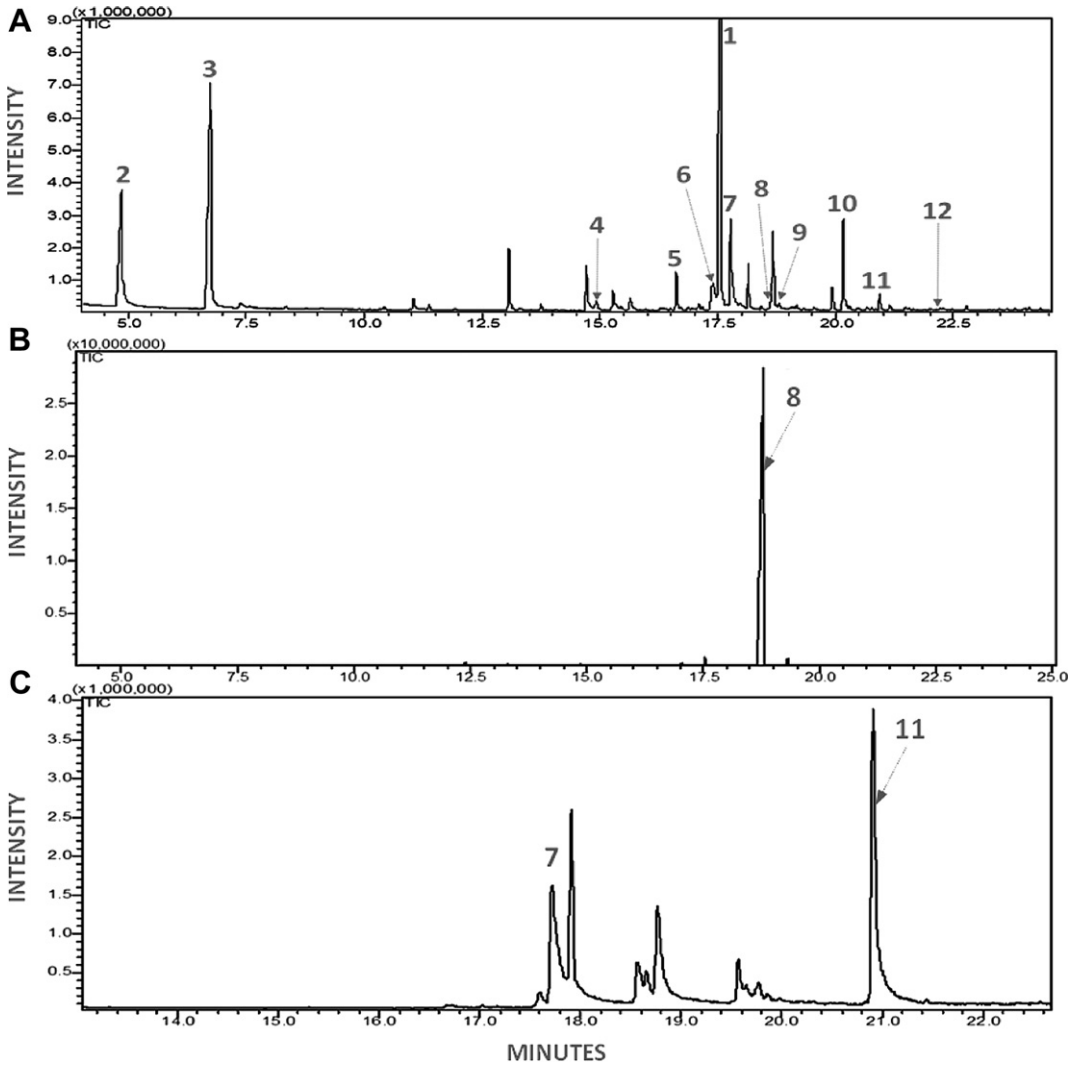


**Fig. 2.** Total ion chromatograms (TIC) of the GC–MS analysis of the *in vitro* oxidation reaction mixtures with the substrate (**A**) lapachol, (**B**) α-lapachone (**8**) and (**C**) dehydro-α-lapachone (**7**) oxidized by iodosylbenzene and Mn(salen). Numbers above the peaks indicate the positions of lapachol (**1**) and respective derivatives (**2**–**12**).

from that, the confirmation of compounds by other spectroscopic techniques was necessary. Therefore an isolation of oxidation products by high performance liquid chromatography coupled to a diode array detector (HPLC-DAD) was aimed, allowing better insights into other compounds generated during catalysis. The chromatographic separation of an upscaled reaction mixture incubated for 24 h led to the isolation of 10 compounds. After purification, reinjection with the GC–MS method and further spectroscopic analysis four additional oxidation products (**6**, **10**–**12**) were identified and previously suggested structures confirmed (Fig. 1). Peak 6 in the GC–MS analysis was shown as an epoxidized derivative of lapachol, 10,11-epoxy-lapachol (**6**), which was a predictable product since the main characteristic of Mn(salen) is the epoxidation of olefinic double bonds as present in the prenyl moiety lapachol (Figs. 1 and 2A). Compound **10** was identified as 2-(1-hydroxy-1-methylethyl)-2,3-dihydronaphtho[2,3-*b*]furan-4,9-dione (**10**), a hydroxylated homologue of the previously identified dehydro-α-isolapachone (**9**). Although peak 11 in the GC–MS chromatogram is not the most intense, the isolation of the respective oxidation product by HPLC-DAD revealed that this is the main oxidation product formed during the performed catalysis conditions. Of the initial lapachol mass, 7.1% are yielded (Table 1) as the hydroxylated pyranic derivative 3,4-dihydro-3-hydroxy-2,2-dimethyl-2*H*-naphtho[2,3-*b*]pyran-5,10-dione (**11**), also commonly known as rinacanthin A. Another oxidation product, compound **12**, isolated in a 5.2% yield from the reaction mixture (Table 1), is one of the few *ortho*-derivatives identified in this type of catalysis with lapachol. Compound **12,** 2-(1-hydroxy-1-methylethyl)-2,3-dihydronaphtho[1,2-*b*]furan-4,5-dione (**12**), is basically the *ortho*-isomer to **10** and despite their similarity they are easily distinguishable by their EI fragmentations. However, possibly due to hydroxyl–group interactions with the stationary phase or small residues and its lower volatility, **12** often exhibited less intense and strongly enlarged signals in TICs of the GC–MS analysis (Fig. 2A). The remaining isolated products were also confirmed by their $^{1}$H NMR spectra as reported in literature (compounds **4**, **5**, **7** and **8**) or by comparison to commercial available references (**3**).

Other noticeable peaks in the TIC of the reaction mixture with lapachol (Fig. 2A), like ones at 13.1 min and 14.8 min, are artifacts of the Mn(salen) and iodosylbenzene which could equally be

**Table 1**
Yields of lapachol oxidation products (**2**–**12**) isolated by HPLC-DAD. Percentage yield values are relative to the initial mass of lapachol as substrate in the catalysis.

| Compound | **2** | **3** | **4** | **5** | **6** | **7** | **8** | **9** | **10** | **11** | **12** |
|---|---|---|---|---|---|---|---|---|---|---|---|
| Yield [%] | – | 4.1 | <1 | 1.7 | 3.3 | 4.2 | <1 | <1 | 4.2 | 7.1 | 5.2 |

observed in blank GC–MS analysis without the substrate (data not shown). Signals at 18.1 min, 18.7 min and 19.9 min (Fig. 2A) presented inconclusive mass spectra, which nevertheless indicated them as being potentially epoxidized or hydroxylated derivatives of lapachol and/or of respective derivatives. However, possibly due to their reactivity and/or instability, the isolation of these compounds did not succeed.

In summary, the compounds identified in the reaction mixture with lapachol indicate a selectivity of Mn(salen) to catalyse *para*-naphtoquinone derivatives, such as compounds **7** or **10** (Fig. 1). Mn(III) porphyrin catalysed oxidations have been shown for such selectivity [9], equally identifying the oxidation products **2**, **3**, **7** and **10** in such reactions. However, *ortho*-naphtoquinone and other types of products, such as norlapachol (**5**), were also detected, suggesting therefore different oxidation mechanisms. Furthermore, Mn(salen) catalysed reactions led in comparison to Mn(III) porphyrin complexes [9] to a higher number of generated and identified compounds, which is advantageous for the prediction and elucidation of the *in vivo* phase I metabolism.

#### 2.1.1. *In vitro oxidation of α-lapachone and dehydro-α-lapachone*

Apart from lapachol itself, two derivatives, dehydro-α-lapachone (**7**) and α-lapachone (**8**), were also briefly studied by the biomimetic model with Mn(salen) and iodosylbenzene in order to understand if those were precursors to oxidation products previously identified. Interestingly the GC–MS analysis of the reaction mixture with **8** revealed that practically none of the α-lapachone is consumed and oxidized into other products (Fig. 2B). Consequently, it can be assumed that the quinone ring double bond in pyranic derivatives of lapachol exhibits an unreactive site for an oxygen transfer by the active Mn(salen) complexes. In contrast, **7** presents a second double bond in the pyran ring, exposing an alternative position for putative interactions with a reactive oxo-manganese(V) complex. As observed in the chromatogram of the catalysis of **7**, several products are formed, of which one was also observed during the prior described biomimetic transformation of lapachol. The hydroxylated derivative **11** identified in both reactions, exhibits the most intense signal among the compounds monitored during the oxidation experiment with **7** (Fig. 2C). Since **7** is in this case the starting substrate we conclude that during the biomimetic oxidation of lapachol, **7** also acts as the precursor to the formation of **11**, possibly via the formation of an epoxidized intermediate.

### 2.2. *Oxidation mechanisms*

As already mentioned in the introduction, metallosalen complexes such as Mn(salen), have the ability to catalyse epoxidation reactions in presence of monooxygen donors such as iodosylbenzene. Two oxidation sites of lapachol are therefore considered possible to receive an oxygen by transfer of the oxomangenese(V) complex: the double bond in the quinone ring and the double bond in the prenyl side chain. Based on compounds (**2**–**12**) identified in the reaction mixture, two competitive oxidation mechanisms were postulated (Fig. 3A and B).

Pathway A initiates with the oxygen transfer to the double bond in the quinone ring of lapachol giving rise to the intermediate **14**, basically in accordance to the first step of the Hooker oxidation [31] (Fig. 3A). In the process of the new ring formation the carbon atom of the original ring attached to the hydroxyl is eliminated as carbon dioxide. A carbon atom of the side chain takes its place and by rearrangement **5** is formed. In accordance to the mechanism postulated by Pires et al. [9], the epoxidation of the prenyl moiety in **14** leads in two steps to the formation of **3** and in one step to compound **2**, which by further oxidation generates a lactone derivative.

In pathway B lapachol epoxidation occurs in the prenyl side chain, which is followed by a tautomeric equilibrium leading to *para*-quinonoid (Pathways B1 and B2) and *ortho*-quinonoid metabolites (pathway B3) (Fig. 3B). All cases therefore are a consequence of intramolecular nucleophilic ring opening of the epoxide. Pathway B1 takes place when hydroxyl addition occurs in the most hindered carbon atom of the epoxide, a pyran ring is formed, resulting in derivative **11**. This hydroxylated derivative is then induced into a hypothetical cycle of dehydration, epoxidation and hydrolysis, leading thereby to the derivative **7**, a theoretic epoxidized intermediate derivative and finally again in **11**. Hydroxyl addition to a less hindered carbon atom of the epoxide **6** (Pathway B2), leads to the hydroxylated homologue **10** of dehydro-α-iso-lapachone (**9**). Further dehydration leads to the formation of **9**. The same heterocyclization mechanism occurred in Pathway B3, leading to the *ortho*-quinonoid nor-ß-lapachone type derivative **12**, which would lead by potential steps of dehydration-oxidation and loss of a 2-propanon unit to the formation of **4**. However, we were not able to identify such precursors of **4**, so that another mechanistic pathway to **4** cannot be excluded. As known from literature [32], lapachol may decompose into α-lapachone in small amounts in solution, by light influence or slightly acidic conditions, such as during the isolation by preparative HPLC, the transformation of lapachol **1** to α-lapachone **8** is also observed during 24 h reactions.

### 2.3. *In vivo analysis of lapachol metabolism*

A non-toxic dose of lapachol (25 mg/kg body weight) was administered to female Wistar rats. At different time-points blood samples were collected after animals' treatment and plasma samples extracted for the identification of lapachol and potential phase I metabolites. The analysis of metabolites was performed by developing a quantitative GC–MS (SIM mode) method with the previously identified oxidation products (**2**–**12**), plus ß-lapachone (**13**). During the analysis the respective characteristic *m/z* ions were monitored (Table 2). External calibrations performed for **1**, **7** and **8** presented respective detection limits at 50 ppb (0.05 μg/mL). Repeatability and linearity was within acceptable ranges of detected concentrations. Because a residual component (fatty acid) of the plasma matrix was interfering in analysis with the elution and monitoring of **8** at 18.58 min (see Fig. 4D), a second temperature gradient (see 4.6, extended SIM method) with an extended runtime was performed in order to clearly assign the derivative **8** at 20.02 min (Fig. 4C).

The analysis of plasma samples evidenced the presence of three compounds, as observed in the respective overlay TIC's for the monitored *m/z* ions of **1**, **7** and **8** (Fig. 4A–C). After 1.5 h a mean plasma concentration for lapachol (**1**) of 37 μg/mL was observed, which successively diminished until a plasma concentration of 2 μg/mL after 12 h (Fig. 5). The derivatives dehydro-α-lapachone (**7**) and α-lapachone (**8**) were also detected, but with clearly lower intensities in TIC's (Fig. 4B and C). Both were detected after 1.5 h with plasma concentrations of 0.6 μg/mL and 1.4 μg/mL, respectively. While **7** was not more detectable after 6 h, compound **8** showed its concentration maximum at 3 h (6.0 μg/mL), which after 12 h decreased to a plasma concentration of 0.7 μg/mL (Fig. 5).

None of the remaining monitored derivatives were detected in the rat plasma samples. In search of other putative metabolites samples were also analysed by GC–MS in Scan mode. However, no other metabolite was identified, either because there simply was no additional derivative of lapachol (**1**) present in samples or because the sensitivity of the GC–MS system in SCAN mode did not allow detecting those (data not shown). However, the results determined that the majority of administered lapachol remains unmetabolized

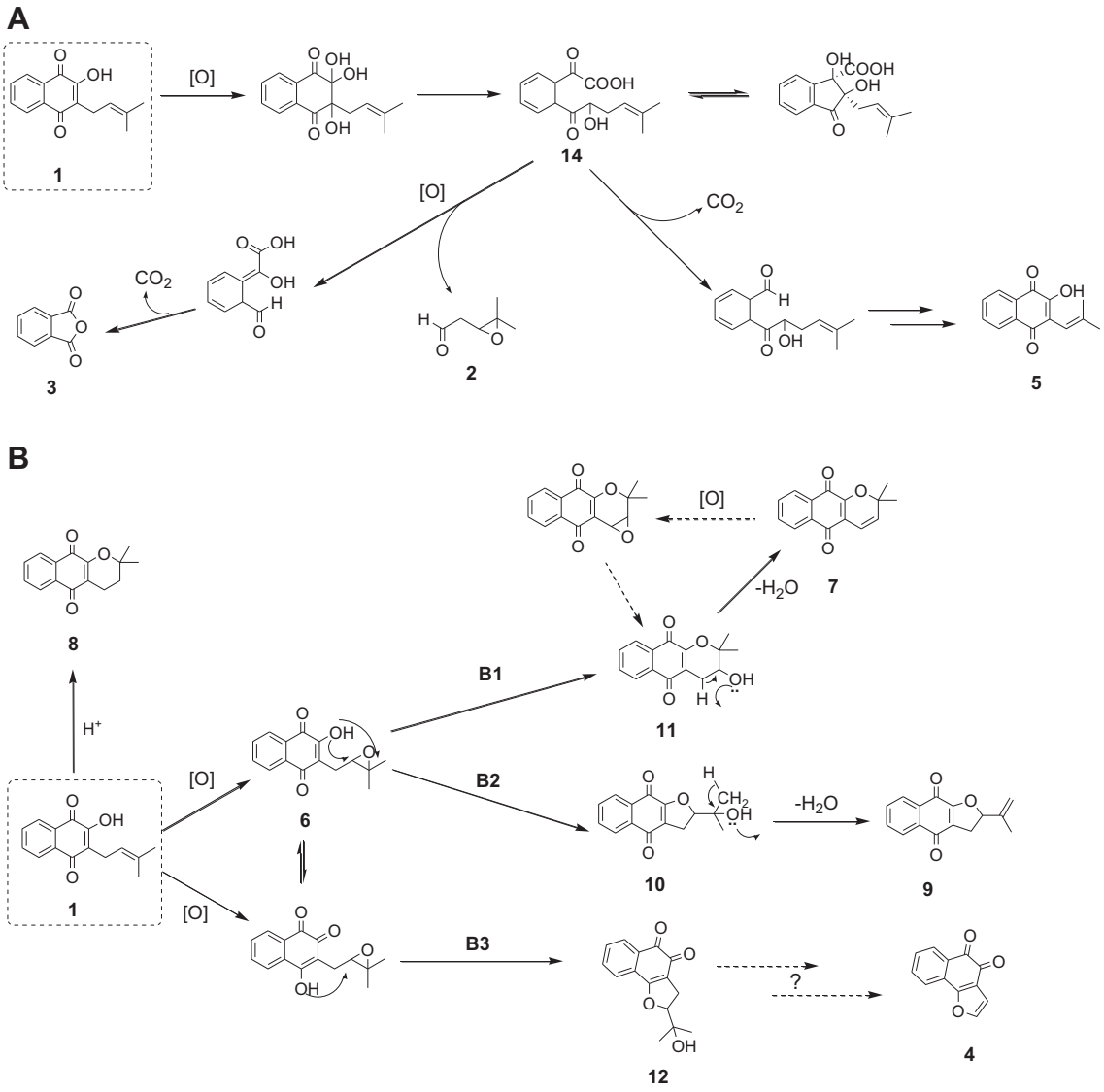


**Fig. 3.** Hypothetical mechanisms for the *in vitro* oxidation of lapachol (**1**) and respective derivatives (**2**–**12**). Pathway **A** shows the mechanism starting with the oxidation of the double bond in the quinone ring of (**1**). Pathway **B** shows the mechanism starting with the oxidation of the double bond in the side chain of (**1**).

after oral administration in rats. In addition, it seems that most of lapachol circulating in the blood stream is eliminated or in another way processed after 12 h, since it is barely detectable in plasma 12 h after administration (Fig. 5). According to the mass spectrometric data, orally administered lapachol is in rats partially converted into the metabolites **7** and **8**. However, lapachol could easily be transformed by cyclization in the acidic environment of the gastric passage to $\alpha$-lapachone (**8**). Hydrochloric acid existent in the human stomach may induce such a reaction [32], so that **8** would not be a genuine phase I metabolite. Dehydro-$\alpha$-lapachone (**7**) on the other hand, has been shown in this study as a genuine oxidation product of lapachol and may therefore also be considered as an *in vivo* oxidation metabolite, probably generated by CYP 450 enzymes mediated catalysis of lapachol. Even though the detected concentration is comparatively low, both compounds should be regarded with interest since different biological activities have been reported for them. $\alpha$-Lapachone (**8**) has for instance shown to inhibit cellular DNA topoisomerase II by a novel mechanism [33] and also demonstrated interesting trypanocidal activity [20]. Dehydro-$\alpha$-lapachone was, for instance, recently reported to exhibit antivascular activity in orthotopic mammary tumors in mice by targeting the cell adhesion [34].

**Table 2**
Compounds and respective ions monitored in the GC–MS (SIM mode) analysis of plasma samples.

| Compound | **1** | **2** | **3** | **4** | **5** | **6** | **7** | **8** | **9** | **10** | **11** | **12** | **14** |
|---|---|---|---|---|---|---|---|---|---|---|---|---|---|
| *m/z* 1 | 199 | 59 | 76 | 114 | 77 | 197 | 197 | 159 | 197 | 144 | 159 | 159 | 159 |
| *m/z* 2 | 227 | 97 | 104 | 142 | 172 | 212 | 225 | 181 | 212 | 172 | 188 | 197 | 214 |
| *m/z* 3 | 242 | 115 | 148 | 170 | 213 | 225 | 240 | 227 | 225 | 200 | 243 | 230 | 227 |
| *m/z* 4 | – | – | – | 198 | 228 | 240 | – | 242 | 240 | 225 | 258 | 258 | 242 |

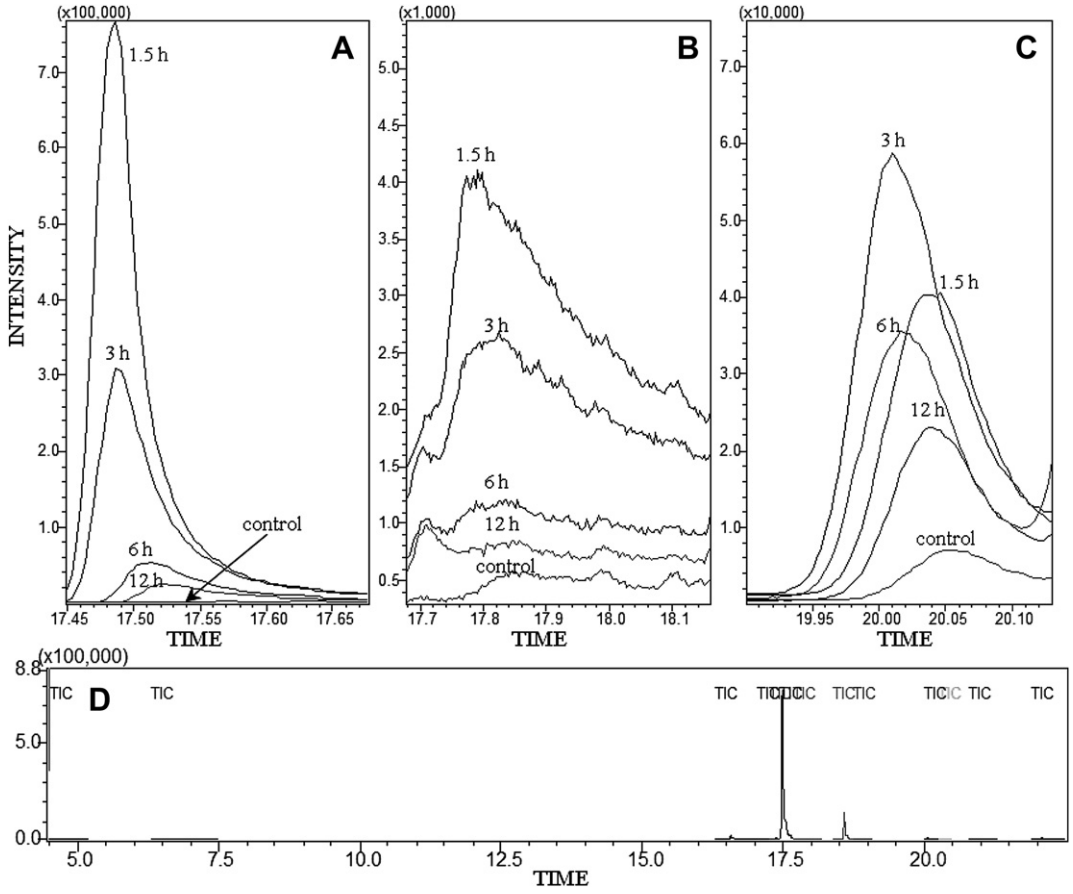


**Fig. 4.** Overlayed TICs from the GC–MS (SIM mode) plasma analyses for the monitored compounds: (**A**) lapachol (**1**), (**B**) dehydro-α-lapachone (**7**) and (**C**) α-lapachone (**8**). **D** presents in summary the TIC's of all signals (see Table 2) monitored in the analysis by GC–MS in SIM mode (total runtime was 37 min).

## 2.4. Experimental data

### 2.4.1. Phtalic anhydride **3** ($C_8H_4O_3$)

$^1$H NMR ($CDCl_3$, 500 MHz) $\delta$ (ppm): 2.17 (s, 1H), 7.97 (s, 3H, 1 $CH_3$), 7.85 (dd, 2H, $J$ = 7.8 Hz and, $J$ = 17.4 Hz, Ar–H). HRESI-MS *m/z* 149.0233 $[M + H]^+$. MS (EI) *m/z* (rel. int., %): 148 (17), 105 (8), 104 (100), 76 (91), 74 (20), 50 (50).

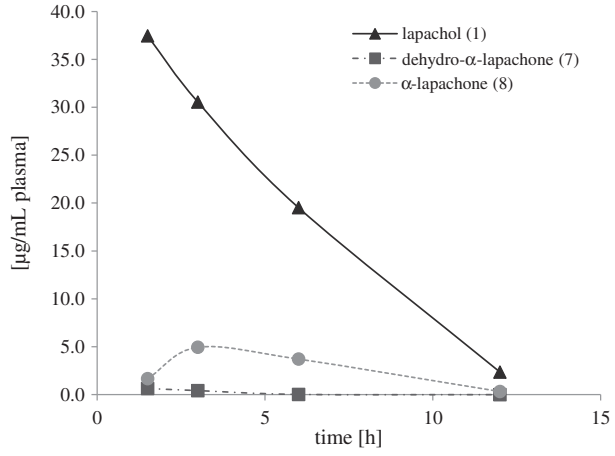


**Fig. 5.** Time-dependent profiles of plasma concentrations for lapachol (**1**), dehydro-α-lapachone (**7**), and α-lapachone (**8**). Quantitative analysis performed by GC–MS (SIM mode). Values are relative to the respective vehicle controls and given as mean ($n$ = 3).

### 2.4.2. Naphtho[1,2-b]furan-4,5-dione **4** ($C_{12}H_6O_3$)

$^1$H NMR (lit. [30]) ($CDCl_3$, 500 MHz) $\delta$ (ppm): 6.83 (d, 1H, $J$ = 2.1 Hz, –CH=) 7.45 (m, 1H, Ar–H) 7.50 (d, 1H, $J$ = 2.1 Hz, –CH=), 7.67 (m, 1H, Ar–H), 7.72 (m, 1H, Ar–H), 8.08 (m, 1H, Ar–H). HRESI-MS *m/z* 199.0437 $[M + H]^+$. MS (EI) *m/z* (rel. int., %): 199 (14), 198 (100), 170 (5), 142 (33), 114 (73), 113 (32), 88 (16), 76 (23), 63 (15).

### 2.4.3. Norlapachol **5** ($C_{14}H_{12}O_3$)

$^1$H-NMR (lit. [38] ($CDCl_3$, 300 MHz)) $\delta$ (ppm): 1.68 (s, 3H, 1 $CH_3$), 1.99 (s, 3H, 1 $CH_3$), 2.17 (s, 1H), 6.00 (s, 1H), 7.69 (m, 1H, Ar–H), 7.76(m, 1H, Ar–H), 8.12 (dd, 2H, $J$ = 7.8 Hz and, $J$ = 17.4 Hz, Ar–H). HRESI-MS *m/z* 229.0878 $[M + H]^+$. MS (EI) *m/z* (rel. int., %): 228 (77), 213 (100), 200 (9), 185 (21), 172 (16), 157 (32), 129 (32), 115 (15), 77 (29).

### 2.4.4. 10,11-Epoxy-lapachol **6** ($C_{15}H_{14}O_4$)

$^1$H NMR (lit. [39]) ($CDCl_3$, 400 MHz) $\delta$ (ppm): 1.23 (s, 3H, 1 $CH_3$), 1.38 (s, 3H, 1 $CH_3$), 1.72 (dd, 1H, $J$ = 4.8 Hz and $J$ = 5.8 Hz, –CH2–), 2.14 (s, 1H, $J$ = 4.8 Hz and $J$ = 5.8 Hz, –CH2–), 2.29 (dd, 1H, $J$ = 5.8 Hz and $J$ = 8.3 Hz, -CH-O), 7.82 (m, 2H, Ar–H), 8.17 (m, 1H, Ar–H), 8.23 (m, 1H, Ar–H). HRESI-MS *m/z* 259.0941 $[M + H]^+$. MS (EI) *m/z* (rel. int., %): 258 (2), 240 (76), 225 (24), 212 (57), 197 (100), 172 (25), 149 (32), 133 (38), 115 (40), 105 (60), 77 (57).

### 2.4.5. Dehydro-α-lapachone **7** ($C_{15}H_{12}O_3$)

$^1$H NMR (lit. [40]) ($CDCl_3$, 500 MHz) $\delta$ (ppm): 1.64 (s, 6H, 2 $CH_3$), 5.81 (d, 1H, $J$ = 10.0 Hz, –CH=), 6.74 (d, 1H, $J$ = 10.0 Hz, –CH=), 7.74–7.81 (m, 2H, ArH), 8.17(d, 2H, $J$ = 7.6 Hz, ArH). HRESI-MS *m/z*

241.0859 $[M + H]^+$. MS (EI) *m/z* (rel. int., %): 240 (11), 225 (100), 212 (5), 197 (30), 133 (8), 115 (14), 105 (16), 76 (18).

*2.4.6. α-Lapachone **8** ($C_{15}H_{14}O_3$)*

$^1$H NMR (lit. [38]) ($CDCl_3$, 500 MHz) δ (ppm): 1.37 (s, 6H, 2 $CH_3$), 1.75 (t, 1H, $J$ = 6.6 Hz, $-CH_2-$), 2.55 (t, 2H, $J$ = 6.6 Hz, $-CH_2-$), 7.61 (t, 2H, $J$ = 7.7 Hz, ArH), 8.01 (m, 2H, ArH). HRESI-MS *m/z* 243.1015 $[M + H]^+$. MS (EI) *m/z* (rel. int., %): 242 (36), 227 (100), 214 (11), 199 (14), 181 (14), 159 (42), 115 (8), 102 (21).

*2.4.7. Dehydro-iso-α-lapachone **9** ($C_{15}H_{14}O_3$)*

$^1$H NMR (lit. [40]) ($CDCl_3$, 400 MHz) δ (ppm): 1.77 (s, 3H, $CH_3$), 3.00 (dd, 1H, $J$ = 9.5 and Hz, $J$ = 17.6 Hz, $-CH_2-$), 3.35 (dd, 1H, $J$ = 11.8 Hz and $J$ = 17.6 Hz, $-CH_2-$) 4.98 (s, 1H, $J$ = 9.5 Hz,$=CH_2$), 5.11 (s, 1H, $=CH_2$), 5.36 (s, 1H, $J$ = 9.5 and $J$ = 11.9 Hz, $-CH_2-$), 7.72(m, 2H, Ar–H), 8.08 (m, 2H, Ar–H). HRESI-MS *m/z* 241.0849 $[M + H^+]$. MS (EI) *m/z* (rel. int., %): 240 (24), 225 (46), 212 (98), 197 (100), 183 (19), 169 (22), 141 (32), 133 (29), 115 (36), 105 (58), 76 (81).

*2.4.8. 2-(1-Hydroxy-1-methylethyl)-2,3-dihydronaphtho[2,3-b] furan-4,9-dione **10** ($C_{15}H_{14}O_4$)*

$^1$H NMR (lit. [38]) ($CDCl_3$, 500 MHz) δ (ppm): 1.34 (s, 3H, $CH_3$), 1.49 (s, 3H, $CH_3$), 3.25 (d, 2H, $J$ = 10.0 Hz, $-CH_2-$) 4.93 (t, 1H, $J$ = 10.0 Hz, –O–CH–) 7.74–7.83 (m, 2H, Ar–H), 8.16 (t, 2H, $J$ = 6.9 Hz, Ar–H). HRESI-MS *m/z* 259.0965 $[M + H]^+$. MS (EI) *m/z* (rel. int., %): 260 (2), 243 (5), 225 (6), 200 (100), 172 (63), 144 (33), 115 (41), 105 (14), 76 (20), 59 (74).

*2.4.9. 3,4-Dihydro-3-hydroxy-2,2-dimethyl-2H-naphtho[2,3-b] pyran-5,10-dione **11** ($C_{15}H_{14}O_4$)*

$^1$H NMR (lit. [40]) ($CDCl_3$, 500 MHz) δ (ppm): 1.44 (s, 3H, $CH_3$), 1.49 (s, 3H, $CH_3$), 2.70 (dd, 1H, $J$ = 5.1 Hz and 18.8 Hz, $-CH_2-$), 2.89 (dd, 1H, $J$ = 5.1 Hz and 18.8 Hz, $-CH_2-$), 3.90 (t, 1H, $J$ = 5.3 Hz, –O–CH–) 7.66-7.75 (m, 2H, Ar–H), 8.11 (dd, 2H, $J$ = 7.5 Hz and $J$ = 13.0 Hz, Ar–H). HRESI-MS *m/z* 259.0965 $[M + H]^+$. MS (EI) *m/z* (rel. int., %): 258 (100), 243 (17), 230 (5), 217 (6), 200 (10), 188 (24), 172 (18), 159 (25), 115 (27), 105 (19), 72 (57).

*2.4.10. 2-(1-Hydroxy-1-methylethyl)-2,3-dihydronaphtho[1,2-b] furan-4,5-dione **12** ($C_{15}H_{14}O_4$)*

$^1$H NMR (lit. [38]) ($CDCl_3$, 500 MHz) δ (ppm): 1.27 (s, 3H, $CH_3$), 1.39 (s, 3H, $CH_3$), 3.06 (d, 2H, $J$ = 9.5 Hz, $-CH_2-$) 4.93 (t, 1H, $J$ = 9.0 Hz, –O–CH–) 7.64–7.69 (m, 1H, Ar–H), 7.73-7.79 (m, 2H, $J$ = 6.9 Hz, Ar–H), 8.11 (d, 2H, $J$ = 7.5 Hz). HRESI-MS *m/z* 259.0965 $[M + H]^+$. MS (EI) *m/z* (rel. int., %): 260 (8), 258 (22), 240 (4), 230 (29), 212 (14), 197 (23), 172 (26), 160 (48), 159 (90), 144 (15), 115 (41), 105 (30), 72 (87).

## 3. Conclusion

The Mn(salen) catalysed oxidation of lapachol resulted in the formation of at least eleven oxidation products, which may be explained bytwo distinct oxidation mechanisms: one starting with the epoxidation of double bond in the quinone ring and the other initiated by oxidation of prenyl side chain of lapachol. The eleven *in vitro* derivatives were used to monitor by GC–MS (SIM mode) metabolites in rat plasma samples. Animals which were orally administered with a non-toxic dosage of lapachol exhibited two metabolites in plasma, α-lapachone (**8**) and dehydro-α-lapachone (**7**). Whereas α-lapachone is probably already formed during the acidic gastric passage and thereupon absorbed, dehydro-α-lapachone is a genuine oxidation metabolite presumably originated by CYP 450 enzymes mediated catalysis. In conclusion, these results show that biomimetic oxidation models, such as the one here presented with an oxomanganese(V) complex as oxygen transfer agent, are an important tool to mimic certain reactions of CYP 450 and therefore also for the prediction and elucidation of the *in vivo* phase I metabolism. The outstanding advantage of such models is the possibility to generate and isolate oxidation derivatives in higher yields at an acceptable cost, such as the ones shown in this study, and by that means have valuable compounds for further toxicological studies as well as for the development and validation of methods for the analysis of *in vivo* metabolites. As reported in previous articles [7,15], this model is also applicable to different classes of bioactive compounds. Furthermore, these systems can help minimizing the use of large animal quantities for *in vivo* metabolism experiments. Although we were able to determine first insights into the oxidative metabolism of lapachol, future and more detailed *in vivo* studies are necessary to fully evidence the metabolism and pharmacokinetic parameters of lapachol and its metabolites.

## 4. Experimental protocols

### 4.1. Chemicals and materials

The Jacobsen catalyst (Mn(salen)), (*S,S*)-(+)-N,N′-Bis(3,5-di-tert-butylsalicylidene)-1,2-cyclohexanediaminomanganese(III) chloride was purchased from Sigma Aldrich, as well as iodosylbenzene diacetate which was used to generate the oxidizing agent iodosylbenzene (PhIO). The synthesis of PhIO was performed according to [35], reaching a purity of 85–90% determined by iodometric titration. Solvents used for *in vitro*, *in vivo* experiments and for the isolation of compounds were of chromatographic grade (Malinckrodt Baker, MXN). Lapachol (**1**) and ß-lapachone (**13**) used for experiments were synthesized and purified according to [36,37]. α-Lapachone (**8**) and dehydro-α-lapachone (**7**) used for biomimetic oxidation reactions were isolated from the correspondent biomimetic catalysis of lapachol.

### 4.2. Biomimetic oxidation with iodosylbenzene and Mn(salen)

In a typical experiment, reactions were carried out in 5 mL vials containing screw caps and under exclusion of light. Mn(salen) (0.5 μmol) and substrate (lapachol, α-lapachone and dehydro-α-lapachone) (15 μmol) were dissolved in acetonitrile to a total volume of 1.5 mL. Thereafter the oxidizing agent PhIO (15 μmol) was added and suspended in acetonitrile. Reaction mixtures were stirred under light exclusion, at constant room temperature over a period of 24 h. After filtration by a 0.45 μm pore size membrane filter, an aliquot was taken for further chromatographic analysis and reaction mixtures then dried under nitrogen flow for storage at −20 °C. The isolation of potential oxidation products was performed with upscaled reactions including up to 150 mg lapachol and applying the previously described proportions.

### 4.3. Oxidation product analysis, isolation and structure elucidation

Generated oxidation products were monitored and analysed by GC–MS (GC-2010, GCMS-QP2010, Shimadzu). A Rtx®-5 MS column (30 × 0.25 mm, 0.25 μm film) (Restek, USA) was used, applying a temperature gradient, 120 °C (4min) → 8 °C/min → 300 °C (12 min), with a total runtime of 37 min. Split injection (1:20) was performed and electron ionization (EI) mass spectra acquired at 70eV.

The isolation of oxidation derivatives from lapachol (**1**) was achieved by a preparative HPLC-DAD method. An RP-C18 column (250 mm × 21.20 mm, 100A, Luna 5 Micron, C18(2), Phenomenex, USA) was employed and chromatographic conditions set for

a 100 min runtime. An appropriate separation of products was achieved by an elution gradient with acetonitrile (A) and purified water (B), both acidified with 1% glacial acetic acid. The elution gradient was as followed: 0.01 min (15% A) → 20 min (30% A) → 30 min (45% A) → 70 (55% A) → 90 min (80%) → 100 min (100% A). Isolated compounds were analysed by high resolution ESI-MS (ultrOTOF$_Q$, Bruker Daltonics) and $^1$H NMR (300 MHz, 400 MHz and 500 MHz, Bruker Daltonics) in order to elucidate and confirm structures.

### 4.4. Lapachol in vivo metabolism

Experiments were carried out on female Wistar rats (*Rattus norvegicus*), weighing approximately 180 g. The animals were acquired from the animal facilities of the Faculdade de Ciências Farmacêuticas de Ribeirão Preto, Universidade de São Paulo, Brazil, and kept in polyethylene boxes ($n = 3$), in a climate-controlled environment with a 12-h, light/dark cycle with free access to water and food. All experiments were conducted in accordance with the guidelines set by the Animal Care Committee (CEUA) of the Universidade de São Paulo, Brazil (Campus of Ribeirão Preto).

The seventeen rats were divided into 6 groups. Lapachol, dissolved in an ethanolic solution (ethanol/water, 1:1) was administered to the rats by oral gavage. In clinical studies, orally administered lapachol was shown to be toxic at doses greater than 2.0 g/day (28.6 mg/kg for a patient of 70-kg body weight) [22]. Therefore, a single administration dose of 0.5 mL with a non-toxic lapachol dose of 25 mg/kg body weight was given and at selected times blood collected by cardiac punction into heparinized tubes. For the treated animals blood was collected after 1.5 h, 3 h, 6 h and 12 h (4 groups, each time point $n = 3$). Animals of the vehicle control group ($n = 4$) were treated with 0.5 mL of the ethanolic solution and for every time period blood of one animal collected. A single Wistar rat was taken for the blank plasma control.

To obtain the plasma, heparinized blood samples were centrifuged at 300 *g* for 15 min and 4 °C, the plasma separated and directly worked up for further GC–MS (SIM mode) analysis.

### 4.5. Metabolite isolation of rat plasma

For the extraction of metabolites from plasma 2 mL methanol were added to 800 μL plasma and mixed vigorously for 5 min. Precipitated proteins were removed by centrifugation at 5000 *g* for 5 min and 4 °C. The methanol supernatant was two times partitioned with 2 mL hexane. The methanol phase was then separated, solvent evaporated under nitrogen atmosphere and the residue dissolved again in 200 μL methanol for GC–MS (SIM mode) analysis. The procedure was validated with defined concentrations of **1**, showing a recovery rate of approximately 95%.

### 4.6. GC–MS (SIM mode) analysis of plasma samples

In order to gain higher sensitivity for the detection of potential phase I metabolites, eleven previously identified oxidation products (**2**–**12**), lapachol (**1**) and *ß*-lapachone (**13**) were used to establish adequate SIM (selective ion monitoring) settings for the GC–MS (SIM mode) analysis. The monitored *m/z* ions in the SIM modus are listed in Table 1. One μL sample volume was injected in splitless mode. The remaining chromatographic conditions were as previously described in 4.3 for the GC analysis of oxidation derivatives from **1**. In order to distinguish **8** at 18.58 min from an interfering matrix residue (fatty acid residue from rat plasma), a second method with an extended temperature gradient was performed (extended SIM method), whereupon compound **8** was detected at 20.02 min. The temperature gradient was as followed: 120 °C (4min) → 8 °C/min → 210 °C (12 min) → 8 °C/min → 300 °C (12 min), with a total runtime of 50 min. Splitless injection of 1 μL and other parameters were as described before.

## Acknowledgements

The authors thank FAPESP, CNPq, INCT_if (CNPq process n° 573663/2008-4) and CAPES (Brazil) for financial support and scholarship.

## Appendix A. Supplementary material

Supplementary material associated with this article can be found, in the online version, at http://dx.doi.org/10.1016/j.ejmech.2012.06.042.

## References

[1] P.R. Ortiz de Montellano, Cytocrome P-450: Structure, Mechanism e Biochemistry, second ed. Plenum Publishers, New York, 2005.
[2] W. Lohmann, U. Karst, Biomimetic modeling of oxidative drug metabolism, Anal. Bioanal. Chem. 391 (2008) 79–96.
[3] J.T. Groves, T.E. Nemo, R.S. Myers, Hydroxylation and epoxidation catalyzed by iron-porphine complexes. Oxygen transfer from iodosylbenzene, J. Am. Chem. Soc. 101 (1979) 1032–1033.
[4] J. Bernadou, B. Meunier, Biomimetic chemical catalysts in the oxidative activation of drugs, Adv. Synth. Catal. 346 (2004) 171–184.
[5] M. Sono, M.P. Roach, E.D. Coulter, J.H. Dawson, Heme-Containing Oxygenases, Chem. Rev. 96 (1996) 2841–2887.
[6] M.C.A.F. Gotardo, L.A.B. Moraes, M.D. Assis, Metalloporphyrins as biomimetic models for cytochrome P-450 in the oxidation of atrazine, J. Agric. Food Chem. 54 (2006) 10011–10018.
[7] T.C.O. Mac Leod, A.L. Faria, V.P. Barros, M.E.C. Queiroz, M.D. Assis, Primidone oxidation catalyzed by metalloporphyrins and Jacobsen catalyst, J. Mol. Cat. A 296 (2008) 54–60.
[8] E. Pfeiffer, C. Herrmann, M. Altemöller, J. Podlech, M. Metzler, Oxidative *in vitro* metabolism of the Alternaria toxins altenuene and isoaltenuene, Mol. Nutr. Food Res. 53 (2009) 452–459.
[9] S.M.G. Pires, R. De Paula, M.M.Q. Simões, A.M.S. Silva, M.R.M. Domingues, I.C.M.S. Santos, M.D. Vargas, V.F. Ferreira, M.G.P.M.S. Neves, J.A.S. Cavaleiro, Novel biomimetic oxidation of lapachol with $H_2O_2$ catalysed by a manganese(III) porphyrin complex, RSC Advances 1 (2011) 1195–1199.
[10] E. Kugelmann, C.R. Albert, G. Bringmann, U. Holzgrabe, Fenton's oxidation: a tool for investigation of potential drug metabolites, J. Pharm. Biomed. Anal. 54 (2011) 1047–1058.
[11] U. Jurva, H.V. Wikström, L. Weidolf, A.P. Bruins, Comparison between electrochemistry/mass spectrometry and cytochrome P450 catalyzed oxidation reactions, Rapid Commun. Mass Spectrom. 17 (2003) 800–810.
[12] T. Katsuki, Mn-salen catalyst, competitor of enzymes, for asymmetric epoxidation, J. Mol. Cat. A: Chem. 113 (1996) 87–107.
[13] D. Feichtinger, D.A. Plattner, Oxygen transfer to manganese–salen complexes: an electrospray tandem mass spectrometric study, J. Chem. Soc. Perkin Trans. 2 (2000) 1023–1028.
[14] D. Feichtinger, D.A. Plattner, Probing the reactivity of Oxomanganese-Salen complexes: an elctrospray tandem mass spectrometry study of highly reactive intermediates, Chem. Eur. J. 7 (2001) 591–599.
[15] M.C. Pigatto, M.C.A. de Lima, S.L. Galdino, I.R. Pitta, R. Vessecchi, M.D. Assis, J.S. dos Santos, T.D. Costa, N.P. Lopes, Metabolism evaluation of the anticancer candidate AC04 by biomimetic oxidative model and rat liver microsomes, Eur. J. Med. Chem. 46 (2011) 4245–4251.
[16] S.G.C. Fonseca, R.M.C. Braga, D.V. Santana, Lapachol – chemistry, pharmacology and assay methods, Rev. Bras. Farm. 84 (2003) 9–16.
[17] K.V. Rao, T.J. McBride, J.J. Oleson, Recognition and evaluation of lapachol as an antitumor agent, Cancer Res. 28 (1968) 1952–1954.
[18] I.T. Palassiano, S.A. De Paulo, N.H. Silva, M.C. Cabral, M.G.C. Carvalho, Demonstration of the lapachol as a potential drug for reducing cancer metastasis, Oncol. Rep. 13 (2005) 329–333.
[19] J.N. Lopes, F.S. Cruz, R. Docampo, M.E. Vasconcelos, M.C.R. Sampaio, A.V. Pinto, B. Gilbert, *In vitro* and *in vivo* evaluation of the toxicity of 1,4-naphtoquinone and 1,2-naphtoquinone derivatives against *Trypanosoma cruzi*, An. Trop. Med. Parasitol. 72 (1978) 523–531.
[20] C. Salas, R.A. Tapia, K. Ciudad, V. Armstrong, M. Orellana, U. Kemmerling, J. Ferreira, J.D. Mayda, A. Morello, *Trypanosoma cruzi*: activities of lapachol and alpha- and beta-lapachone derivatives against epimastigote and trypomastigote forms, Bioorg. Med. Chem. 16 (2008) 668–674.
[21] T.L. Lemos, F.J. Monte, A.K. Santos, A.M. Fonseca, H.S. Santos, M.F. Oliveira, S.M. Costa, O.D. Pessoa, R. Braz-Filho, Quinones from plants of northeastern Brazil: structural diversity, chemical transformations, NMR data and biological activities, Nat. Prod. Res. 20 (2007) 529–550.

[22] J.B. Block, A.A. Serpick, W. Miller, P.H. Wiernik, Early clinical studies with Lapachol (NSC-11905), Cancer Chemther. Report Part 2 (4) (1974) 27–28.
[23] M.N. Da Silva, V.F. Ferreira, M.C.B.V. De Souza, An overview of the the chemistry and pharmacology of naphtoquinones with emphasis on ß-lapachone and derivatives, Quím. Nova 26 (2003) 407–416.
[24] T.J. Monks, R.P. Hazlik, G.M. Cohen, D. Ross, D.G. Graham, Quinone chemistry and toxicology, Toxicol. Appl. Pharmacol. 112 (1992) 2–16.
[25] J.L. Bolton, M.A. Trush, T.M. Penning, G. Dryhurst, T.J. Monks, Role of quinones in toxicology, Chem. Res. Toxicol. 13 (2000) 135–160.
[26] C.A. Camara, A.C. Pinto, M.A. Rosa, M.D. Vargas, Secondary amines and unexpected 1-aza-anthraquinones from 2-methoxylapachol, Tetrahed. 57 (2001) 9569–9574.
[27] T.M. Silva, C.A. Camara, T.P. Barbosa, A.Z. Soares, L.C. da Cunha, A.C. Pinto, M.D. Vargas, Molluscicidal activity of synthetic lapachol amino and hydrogentaed derivatives, Bioorg. Med. Chem. 3 (2005) 193–196.
[28] C.O. Salas, M. Faúndez, A. Morello, J.D. Maya, R.A. Tapia, Natural and synthetic naphtoquinones active against *Trypanosoma cruzi*: an initial step towards new drugs for Chagas disease, Curr. Med. Chem. 18 (2011) 114–161.
[29] M. Girard, J.-C. Ethier, D. Kindack, B.A. Dawson, D.V.C. Awang, Mass spectral characterization of naphtoquinones related to lapachol, J. Nat. Prod. 50 (1987) 1149–1151.
[30] D.C. Sutton, F.T. Gillan, M. Susic, Napthofuranone Phytoalexins from the grey Mangrove *Avicennia marina*, Phytochem 24 (1985) 2877–2879.
[31] S.C. Hooker, The consitution of lapachol and its derivatives. Part IV. Oxidation with potassium permangante, J. Am. Chem. Soc. 58 (1936) 1168–1173.
[32] S.C. Hooker, The consitution of lapachol and its derivatives. Part V. The structure of Paterno's Isolapachone, J. Am. Chem. Soc. 58 (1936) 1190–1197.
[33] P. Krishnan, K. Bastow, Novel mechanism of cellular DNA topoisomerase II inhibition by the pyronaphtoquinone derivatives $\alpha$-lapachone and $\beta$-lapachone, Cancer Chemother. Pharmacol. 47 (2001) 187–198.
[34] I. Garkavtsev, V.P. Chauhan, H.K. Wong, A. Mukhopadhyay, M.A. Glicksman, R.T. Peterson, R.K. Jain, Deydro-α-lapachone, a plant product with antivascular activity, PNAS (2011) 11596–11601.
[35] H. Saltzmann, J.G. Sharefkin, Iodosylbenzene, Org. Synth. 5 (1973) 658.
[36] S.B. Ferreira, D.R. Rocha, J.W.M. Carneiro, W.C. Santos, V.F. Ferreira, A new method to prepare 3-alkyl-2-hydroxy-1,4-naphthoquinones: synthesis of lapachol and phthiocol, Synlett 11 (2011) 1551–1554.
[37] S.C. Hooker. LVII, The constitution of lapachic acid (lapachol) and derivatives, J. Am. Chem. Soc. Trans. 61 (1892) 611–654.
[38] E.P. Sacau, A. Estévez-Braun, A.G. Ravelo, E.A. Ferro, H. Tokuda, T. Mukainaka, H. Nishino, Inhibitory effects of lapachol derivatives on Epstein-Barr virus activation, Bioorg. Med. Chem. 11 (2003) 483–488.
[39] C.M.R. Ribeiro, P.P. de Souza, L.L.D.M. Ferreira, S.L. Pereira, I.S. Martins, R.A. Epifanio, L.V. Costa-Lotufo, P.C. Jimenez, C. Pessoa, M.O. de Moraes, Natural furano naphtoquinones from lapachol: hydroxyiso-ß-lapachone, stenocarpoquinone-B and avicequinone-C, Lett. Org. Chem. 8 (2011) 347–351.
[40] C.M.R. Ribeiro, P.P. de Souza, L.L.D.M. Ferreira, L.A. Pinto, L.S. de Almeida, Janaina G. de Jesus. Cyclization of lapachol induced by thallium salts, Quim. Nova 31 (2008) 759–762.